

Chapter 10

Direct Numerical Simulation of Autoignition in Turbulent Non-premixed Combustion

Kedar G. Bhide and S. Sreedhara

Abstract Combustion in a CI engine is initiated by self-ignition of fuel–air mixture caused by high pressure and high temperature; a process known as autoignition. Autoignition is a challenging problem to simulate as the temperature increases from initial temperature to the adiabatic flame temperature in a very short duration. Numerical study of a turbulent flow using RANS/LES encounters a closure problem. Accuracy of closure models can be improved through experimental results, theoretical reasoning and direct numerical simulation (DNS) data. A review of DNS of autoignition in a turbulent non-premixed medium is presented in this chapter. As observed from DNS study, autoignition sites in a turbulent non-premixed medium are not randomly distributed but follow a pattern in the mixture fraction-scalar dissipation rate space. Turbulent flow is always three-dimensional in nature. 2D DNS of autoignition shows that ignition delay time increases with increase in initial turbulence intensity, which contradicts with the experimental observation. 3D DNS of autoignition resolves this conflict. The conflict is mainly due to the absence of vortex-stretching phenomenon in 2D DNS. Homogeneous charge compression ignition (HCCI) is being considered as one of the strategies toward improving performance of conventional CI engines. However, HCCI engines suffer from drawbacks like lack of control over combustion and limited operating regime. One of the modifications suggested in the HCCI technology to overcome these drawbacks is the use of stratification in the fuel–air mixture. Therefore, a few DNS studies on autoignition in the stratified medium have been discussed here. Further, discussion on the conditional moment closure (CMC) model and its validation using DNS data has been presented. Ignition delay time predicted by CMC was found to be in good agreement with DNS predictions.

Keywords DNS · Autoignition · CMC · HCCI · Charge stratification

K. G. Bhide · S. Sreedhara (✉)

IC Engines and Combustion Laboratory, Mechanical Engineering Department, Indian Institute of Technology Bombay, Mumbai 400076, India
e-mail: sreedhara.s@iitb.ac.in

Abbreviations

CFD	Computational Fluid Dynamics
CI	Compression Ignition
CMC	Conditional Moment Closure
DNS	Direct Numerical Simulation
HCCI	Homogeneous Charge Compression Ignition
HRR	Heat Release Rate
LES	Large Eddy Simulation
MR	Most Reactive
RANS	Reynolds-Averaged Navier–Stokes
SI	Spark Ignition
TDC	Top Dead Center
2D/3D	Two Dimensional/Three Dimensional

Nomenclature

c_p	Specific heat at constant pressure
D	Fickian diffusion coefficient
Da	Damköhler Number
E_a	Activation energy of a reaction
h_r	Heat of reaction
Δh_α	Heat of formation of a species
H_F	Heat of combustion of fuel
N_S	Number of species
$Q(\eta; x, t)$	Conditional average of any scalar Y on $\xi = \eta$
R	Universal gas constant
T	Temperature
T_a	Activation temperature of a reaction (E_a/R)
T_{in}	Initial Temperature
u_{rms}	Root mean square value of velocity fluctuations
Y_i	Mass fraction of i th species
α, β	Indices of species
η	Sample space of ξ
θ	Excess temperature given by $(T - T_{in})c_p/h_r$
λ	Thermal Diffusivity
ξ	Mixture fraction (Eq. 2)
ρ	Density
σ^2	Conditional variance of excess temperature θ
τ_{ign}	Ignition delay
τ_t	Integral timescale of turbulence
τ_0	Ignition delay in homogeneous mixture (or other reference timescale)
$\varphi_{\alpha\beta}$	Factor defined by Eq. 11
χ	Scalar dissipation rate (Eq. 1)
$\dot{\omega}_i$	Chemical source term of i th species

Λ	Integral length scale of turbulence
Λ_k	Kolmogorov scale of turbulence
Λ_ξ	Integral scale of initial scalar distribution
\mathcal{V}	Vortex locating index (Sect. 10.2.1)

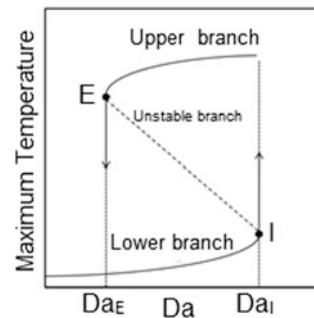
10.1 Introduction

Combustion in practical devices like internal combustion engine, gas turbine takes place in a turbulent medium. Combustion in these devices can be initiated by (a) an external source, like in spark ignition (SI) engine or (b) self-ignition or autoignition, like in compression ignition (CI) engine. In CI engines, fuel is injected close to the top dead center (TDC) during compression stroke. Pressure and temperature of the air inside the cylinder at the time of injection is high (40–60 bar, 700–1000 K (Heywood 1988)). The fuel injected at this point through the injector atomises into smaller droplets and these droplets vaporize. Vaporized fuel mixes with surrounding hot and high pressure air. Due to high temperature and pressure, pockets of well-mixed fuel–air mixture undergo autoignition characterized by heat release which increases temperature and pressure in the chamber. This further facilitates vaporization of the incoming fuel (Heywood 1988). No external source is required to start the combustion. High temperature and pressure of air is sufficient to start the ignition once the fuel and air are mixed in the appropriate proportion. Nonlinear dependence of rate of reaction on temperature, through Arrhenius expression, is well-known. If the initial temperature, T_0 , of fuel–air mixture is high enough to start a small reaction which generates heat, then this heat further increases the temperature of the mixture by a small amount. Increased temperature further accelerates the heat release. Temperature of the mixture increases rapidly after certain point in time and this process is known as autoignition (Mastorakos 2009). Ignition delay is an important parameter and is defined as the time between the start of injection and the start of combustion. Several definitions may be used to define the start of combustion, for example, the time of peak heat release. It is of the order of a *ms* in CI engines (Heywood 1988). Apart from CI engines, autoignition plays an important role in stabilizing turbulent jet flames with vitiated coflow as shown experimentally by Cabra et al. (2006).

Study of a perfectly mixed fuel–air mixture at initial temperature T_0 represents a zero dimensional study which ignores the effects of fluid dynamics on autoignition. Numerical (for example, Im et al. 2000) as well as experimental (for example, Fotache et al. 1997) studies help to understand fluid dynamic effects. Opposed jet flow configuration was generally used in many such studies. Fotache et al. (1997) in the experimental study of methane–air ignition observed that the temperature of the

air stream required for autoignition to occur, increased monotonically with increasing strain rate. Strain rate was calculated as the maximum gradient of axial velocity. Strain rate was considered as the inverse of characteristic flow timescale (Im et al. 2000). Strain rate was varied by varying fuel and oxidizer velocities. Im et al. (2000), in a numerical study, also observed that ignition delay increased with increasing strain rate. Beyond a certain value of the strain rate, called steady ignition limit, ignition did not occur. This dependence of ignition temperature or ignition delay on the strain rate is explained using a classical S-curve shown in Fig. 10.1 (Peters 2004). Ratio of characteristic flow timescale to the characteristic chemical timescale is known as Damköhler number (Da). As Da increases along the lower branch (increase in characteristic flow time), maximum temperature in the domain increases. At the critical point I, maximum temperature suddenly increases signifying a successful autoignition. Autoignition is not possible below this critical value Da_I . If one starts from higher branch and reduces Da , at the critical point E, maximum temperature suddenly drops indicating extinction of the flame. Im et al. (1999), in a numerical study, observed the influence of an unsteady velocity field on opposed jet diffusion flame. Scalar dissipation rate was proposed as another factor to represent the characteristic flow timescale. Scalar dissipation rate and strain rate were found to be correlated well with the change in imposed flow velocity. When an oscillating velocity field was imposed, the scalar dissipation rate was found to follow oscillating field better than the strain rate followed. Expression for scalar dissipation rate is given by Eq. (1), where λ denotes thermal diffusivity and ξ represents mixture fraction. Mixture fraction represents local fuel-oxidizer ratio and it changes from 0 in pure oxidizer to 1 in pure fuel. Transport equation of ξ does not contain a reaction term so it is defined appropriately based on the chemistry used in a study. For a single-step chemistry, ξ is defined as given by Eq. (2). $\beta = Y_F - r_{st}Y_O$, where Y_F and Y_O are fuel and oxidizer mass fractions respectively. r_{st} is the ratio of mass of fuel to that of oxidizer in the stoichiometric mixture. High value of the scalar dissipation rate indicates high diffusive losses of species/temperature from a given location. Dimension of the scalar dissipation rate is s^{-1} and hence, local flow timescale can be taken to be low at the location of high scalar dissipation

Fig. 10.1 S-curve showing a variation of maximum temperature in a well-stirred reactor with Damköhler number (Peters 2004)



rate. According to classical S-curve, autoignition may not be favored at such locations due to Da being smaller than the critical value, Da_c .

$$\chi = 2\lambda \left(\frac{\partial \xi}{\partial x} \right) \left(\frac{\partial \xi}{\partial x} \right) \quad (1)$$

$$\xi(x, t) = \frac{\beta(x, t) - \beta_{air}}{\beta_{fuel} - \beta_{air}} \quad (2)$$

As stated previously, combustion in practical devices takes place in a turbulent medium. In CI engines, turbulence affects atomization, vaporization, and mixing of fuel and air prior to the onset of autoignition. Experimental study by Mizutani et al. (1990) using shock tube demonstrated that turbulence promoted mixing of fuel–air and autoignition of column of cetane droplets occurred at 840 K and 10 bar that required a temperature of 1100 K to autoignite in the absence of turbulence. Ignition delay was also reduced with increase in turbulence intensity. However, still higher value of turbulence may inhibit autoignition by promoting heat loss from the igniting mixture. Therefore, the study of autoignition in a turbulent non-premixed medium becomes very important.

10.1.1 Numerical Modeling of Autoignition

Development of advanced CFD techniques along with upgraded computational facilities have allowed numerical study of not just autoignition but also of large number of turbulent reacting flows. Numerical approaches used for such studies and for turbulent flows in general are Reynolds-Averaged Navier–Stokes (RANS), large eddy simulation (LES), and direct numerical simulation (DNS). It is well known that details of the solution obtained at the end increase from RANS to DNS, but computational effort and grid resolution required also increase in the same order. RANS and LES suffer from closure problems where closure models are required for some of the terms in the governing equations. DNS approach tries to capture all the fluctuations of a variable at a point. Instantaneous, full set of Navier–Stokes equations are solved without using any closure models. Hence, DNS studies can be used to assess the accuracy of closure models used in the RANS/LES. Models used in the RANS/LES of non-premixed combustion have been discussed in the textbook by Poinso and Veyante (2005).

Liñán and Crespo (1976) investigated autoignition in one-dimensional laminar mixing layer and introduced the concept of “most reactive mixture fraction”, denoted as ξ_{MR} . This theory has been found to be valid under turbulent conditions also as seen from the DNS studies discussed in this chapter. The theory states that reaction starts at a location where mixture fraction ξ has attained the value of ξ_{MR} . It

may be understood qualitatively by using a single-step, second-order reaction. Rate of fuel consumption in such a reaction in terms of ξ is given by Eq. (3).

$$\dot{\omega}_F \propto \xi(1 - \xi) \exp \left[\frac{-T_a}{T_{air} - \xi(T_{air} - T_F)} \right] \quad (3)$$

When T_{air} is equal to T_F , rate of fuel consumption reaches maximum at $\xi = 0.5$. When $T_{air} > T_F$, the exponential dependence of fuel consumption on temperature causes the peak to shift toward leaner and hotter ($\xi < 0.5$) mixtures. This value of ξ could be other than the stoichiometric mixture fraction ξ_{st} . Thus, the value of ξ_{MR} , where fuel consumption reaches maximum, is decided by T_a , T_{air} , and T_F in a second-order reaction.

10.2 Direct Numerical Simulation

As discussed in the previous section, DNS tries to capture all the fluctuations in a variable at a point. It requires a domain to be large enough to resolve large scales and a mesh to be fine enough to resolve smallest of the scales. In a domain of size L that has been discretized into N points in each direction, cell size becomes $\Delta x = L/N$. Domain length L should be greater than the integral scale Λ and the mesh size Δx should be smaller than the Kolmogorov scale Λ_k . Combination of these restrictions leads to a criterion that determines the highest turbulent Reynolds number flow that can be solved using a given mesh size (Poinso and Veyante 2005). It is given by Eq. (4). Re_T is defined based on Λ and u_{rms} . In addition to scales of turbulence, important length scales of combustion, such as flame thickness, should be resolved properly by the grid size used in a DNS study.

$$Re_T < N^{4/3} \quad (4)$$

A mesh size of the order of microns is often used in DNS studies. Such a small mesh size takes the total number of grid points over a million even in a domain size of a few mm^3 . Such a large number of grid points pose challenges to computation time as well as storage. DNS of real scale geometries is not yet possible due to these challenges. Therefore, DNS is usually carried out over a cubic domain where temperature, pressure, fuel distribution, and flow timescale are representative of practical devices. In addition to a small mesh size, DNS demands smaller time step to capture wide range of timescales. Explicit time stepping is often used in DNS and time step is decided by the conventional Courant–Friedrich–Lewy (CFL) number (Moin and Mahesh 1998). In a reacting flow, chemical timescales may be smaller than flow timescales. In such a scenario, fractional time stepping method may be used. A smaller time step for reaction terms and a larger time step for flow may be used in this technique (for example, Sreedhara and Lakshmisha 2000).

Fig. 10.2 Use of DNS in solving industrial problems like IC engines

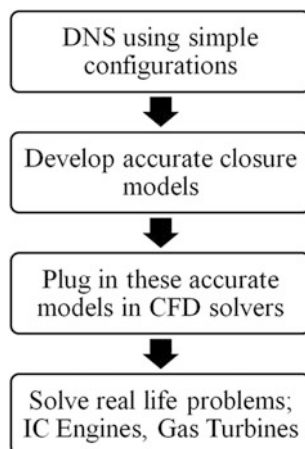


Figure 10.2 shows the steps in developing new closure models using DNS and finally plugging these accurate closure models in commercial CFD packages to solve industrial problems. RANS simulations do not capture turbulent fluctuations and calculate only the averaged field. LES captures only large-scale fluctuations. Therefore, the effect of turbulent fluctuations and the effect of small-scale fluctuations need to be modeled in RANS and LES studies, respectively. This is known as a closure problem. Since DNS captures all scales of turbulent fluctuations, data obtained from the DNS may be used to assess the accuracy of existing closure models or to build new closure models. Assessment of accuracy of the CMC model has been discussed in Sect. 10.4 of this chapter.

10.2.1 DNS Studies of Autoignition

DNS studies of autoignition in a turbulent non-premixed medium have been reviewed in this section. Different configurations have been used by several authors. These configurations are provided in Table 10.1.

In an early two-dimensional (2D) DNS study, Mastorakos et al. (1997) simulated the autoignition of CH₄-air mixture using a single-step chemistry. This study revealed some of the fundamental aspects of autoignition in a turbulent medium, which have been confirmed by 3D DNS and using multistep chemistry in later studies. This study concluded that the autoignition in turbulent non-premixed medium occurs at a location where (a) mixture fraction has attained a value of most reactive mixture fraction and (b) conditional scalar dissipation rate is low. This aspect has been better explained by taking joint conditional mean of reaction rate conditioned on mixture fraction and scalar dissipation rate ($\langle \dot{\omega}_F | \xi, \chi \rangle$) by Sreedhara and Lakshmisha (2000) and is shown in Fig. 10.3a. It should be noted that the study

Table 10.1 Configurations considered in the DNS of autoignition

Author	Description
Mastorakos et al. (1997)	(a) Shearless mixing layer between fuel and air (b) Fuel slab surrounded by air on two sides
Sreedhara and Lakshmisha (2000, 2002a)	Parcels of relatively colder fuel dispersed randomly in the hot surrounding air
Yoo et al. (2011)	Fuel jet surrounded by highly heated coflow of air

of Sreedhara and Lakshmisha (2000) used a different configuration as shown in Table 10.1. In another study, Sreedhara and Lakshmisha (2002a) performed a 3D DNS of autoignition using single-step chemistry of *n*-Heptane–air. They observed that, similar to a 2D DNS, autoignition spots in a 3D DNS occur at a location where low conditional scalar dissipation rate and most reactive mixture fraction are jointly present. However, they also mentioned that for a multistep chemistry, it is not possible to have a unique value of ξ_{MR} . This was attributed to the different activation energies of different reactions which are active during the stages of combustion. Mastorakos et al. (1997) also observed that the turbulent flow ignited earlier than the laminar flow. It was proposed that since turbulence creates wide range of $\chi|\xi_{MR}$ (conditional scalar dissipation rate conditioned on most reactive mixture fraction), there exist some regions where $\chi_{turb}|\xi_{MR}$ is smaller than $\chi_{lam}|\xi_{MR}$. Such regions ignite earlier in turbulent flow. Partial premixing in the presence of turbulence also reduced the ignition delay. Partial premixing reduces $\partial\xi/\partial x$ and thus $\chi|\xi_{MR}$ which causes earlier ignition. A fuel slab of finite width surrounded by air on both sides showed earlier ignition compared to shearless mixing layer case in this study. Also, delay increased with increasing width of the slab. Lower width resulted in faster decay of $\chi|\xi_{MR}$ through faster mixing and ignited earlier. Mukhopadhyay and Abraham (2012) studied the autoignition of *n*-Heptane–air mixing layer using multistep chemistry capable of capturing two-stage ignition of *n*-Heptane. Two-stage autoignition of *n*-Heptane has been illustrated in Fig. 10.6. Autoignition in a turbulent medium was observed to occur earlier than in a laminar medium. Only high temperature autoignition was influenced by turbulence. Heat release from a low temperature ignition showed a weak negative correlation with the scalar dissipation rate, whereas high temperature autoignition was observed to occur at the location of low scalar dissipation rate. Yoo et al. (2011) studied the role of autoignition in stabilizing a lifted jet flame surrounded by hot coflow. Flame height showed a sawtooth variation with time characterized by a slow movement in the downstream direction and a sudden movement in the upstream direction. DNS data showed that sudden drop in the flame height occurs simultaneously with reducing scalar dissipation rate. Contours of OH showed igniting kernels near the exit of the jet. These kernels reduce the flame height. Kernels are eventually convected downstream by high axial jet velocity. This explains the sawtooth movement of the flame height.

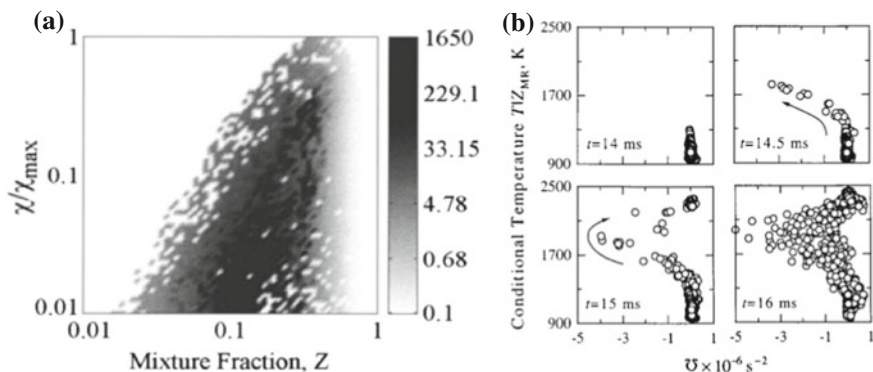


Fig. 10.3 **a** Joint conditional mean of reaction rate ($\langle \dot{\omega}_F | \xi, \chi \rangle$) at the instant of first appearance of autoignition spots **b** scatter plot of $T|_{\xi_{MR}}$ and vortex location index $\bar{\mathcal{U}}$ at different times around first appearance of ignition spots. Both pictures are reprinted from Sreedhara and Lakshmisha (2000), by permission of the Combustion Institute

Sreedhara and Lakshmisha (2000, 2002a) further examined the location of autoignition spots relative to vortical structures. A new Index $\bar{\mathcal{U}}$ was defined that shows whether a location belongs to a vorticity dominated core ($\bar{\mathcal{U}} < 0$) or a strain-dominated tail ($\bar{\mathcal{U}} > 0$) regions. Temperature conditioned at most reactive mixture fraction is plotted as a function of $\bar{\mathcal{U}}$ in Fig. 10.3b. As shown in Fig. 10.3b, the reaction starts at 14.5 ms in the core region where strain rate is low (hence low χ). During vigorous burning stage, hot gases move toward the strain-dominated tail region (15 ms). The constant density simulation did not show such a movement of autoignition spots in T - $\bar{\mathcal{U}}$ plane. Autoignition occurred in core as well as in tail regions with equal probability when constant density was assumed. Therefore, density fluctuations were considered to be responsible for this movement of autoignition spots in T - $\bar{\mathcal{U}}$ plane. Krisman et al. (2017) recently studied the autoignition in a temporally evolving planar jet of *n*-Heptane in a stationary layer of air at high pressure using 3D DNS. Four-step chemistry capable of reproducing two-stage ignition of *n*-Heptane was used. Low temperature heat release was found to occur in strain-dominated regions of vortices. High temperature ignition was found to occur in the vorticity dominated core regions of vortices. Different criteria were used by Sreedhara and Lakshmisha (2000) and Krisman et al. (2017) to determine the local vortical structures in their respective studies.

In another 2D DNS study, Krisman et al. (2016) studied the two-stage ignition of dimethyl ether in a shearless mixing layer. Low temperature ignition was observed to occur at a location where mixture fraction is leaner than stoichiometric and the scalar dissipation rate is low. Strong negative correlation of heat release in the low temperature ignition with the scalar dissipation rate was observed. This low temperature ignition initiated a diffusively supported flame or deflagration, which traveled toward richer values of mixture fraction. This passage of diffusively supported flame was found to affect the high temperature ignition.

10.2.1.1 Influence of Turbulence Parameters on Ignition Delay

Im et al. (1998), Hilbert and Thevenin (2002), and Sreedhara and Lakshmisha (2000, 2002a) studied the influence of various turbulence parameters on autoignition in a turbulent non-premixed medium using DNS. These parameters include intensity of turbulence (u_{rms}), integral scale of turbulence (Λ), integral timescale of turbulence ($\tau_t = \Lambda/u_{rms}$) and integral scale of initial scalar distribution (Λ_ξ). Im et al. (1998) performed 2D DNS of hydrogen–air mixing layer. Ignition delay for laminar case (τ_0) was used as a reference timescale. Three levels of turbulence were studied by changing Λ such that $\tau_t/\tau_0 \approx 0.3, 1, \text{ and } 3$. For $\tau_t/\tau_0 \geq 1$, ignition delay (τ_{ign}) was found to be unaffected by change in τ_t . However, for $\tau_t/\tau_0 \approx 0.3$, increase in τ_{ign} was observed compared to previous two cases. Hilbert and Thevenin (2002) in a 2D DNS study changed Λ and u_{rms} simultaneously so that τ_t remained constant and τ_t/τ_0 was equal to 2. τ_{ign} was found to be independent of changes in Λ and u_{rms} in this study. Using 2D DNS, Sreedhara and Lakshmisha (Sreedhara and Lakshmisha 2000) studied the effect of Λ_ξ , in addition to τ_t , on τ_{ign} . Change in τ_t was brought about by changing u_{rms} . All the cases considered in this study had $\tau_t/\tau_0 > 1$ (τ_0 represents ignition delay corresponding to a homogeneous mixture). Ignition delay was found to increase with decrease in τ_t when the ratio Λ_ξ/Λ was greater than 1. However, it became independent of τ_t when the ratio Λ_ξ/Λ was less than 1. This dependence was clearly explained based on the variation of $\chi|\xi_{MR}$ with time. When the ratio Λ_ξ/Λ was greater than 1, faster turbulence (lower τ_t) resulted in higher value of $\chi|\xi_{MR}$ and thus delayed the ignition. When the ratio Λ_ξ/Λ was less than 1, all curves showing variation of $\chi|\xi_{MR}$ with time nearly collapsed together resulting in similar values of τ_{ign} independent of τ_t . Sreedhara and Lakshmisha (2002a) in a 3D DNS study comprehensively studied the effect of turbulence parameters on τ_{ign} . When the ratio Λ_ξ/Λ was less than 1 and τ_t/τ_0 was low, τ_{ign} decreased with faster turbulence. However, the effect of τ_t on τ_{ign} diminished with increasing τ_t/τ_0 . However, when $\tau_t/\tau_0 \approx 1$, the ratio $\Lambda_\xi/\Lambda > 1$ made effect of τ_t more pronounced compared to the case where $\Lambda_\xi/\Lambda < 1$. Based on this 3D study, influence of different parameters can be summarized as in Table 10.2. Two regimes of autoignition are possible (a) mixing controlled and (b) kinetics controlled (Sreedhara 2002). When the ratio τ_t/τ_0 was low, mixing of fuel with air controlled the rate of reaction. Faster turbulence facilitated this enhanced mixing and decreased the ignition delay. In kinetics controlled regime ($\tau_t/\tau_0 \approx 1$), mixing is not the rate limiting process. A few well-mixed spots were sufficient to start the ignition.

Table 10.2 Influence of decreasing τ_t on τ_{ign} based on 3D DNS

	$\tau_t > \tau_0$	$\tau_t < \tau_0$
$\Lambda_\xi/\Lambda < 1$	Largely unaffected	τ_{ign} decreases with decreasing τ_t
$\Lambda_\xi/\Lambda > 1$	τ_{ign} decreases with decreasing τ_t	Case not considered

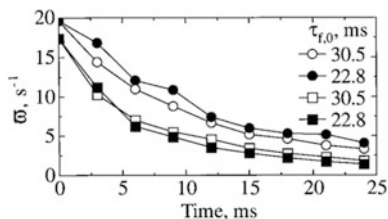


Fig. 10.4 Variation of ϖ with time in 2D (●, ○) and 3D (■, □) simulation. τ_t denoted by $\tau_{f,0}$ in this figure. Reprinted from Sreedhara and Lakshmisha (2002), by permission of the Combustion Institute

Effect of dimensionality (2D/3D) of DNS on the influence of τ_t on autoignition was also studied by Sreedhara and Lakshmisha (2002a). The 2D case ignited later than the 3D case for the same initial conditions. Also in 2D case, τ_{ign} increased with decreasing τ_t contrary to 3D cases discussed above. Increasing u_{rms} strengthens two opposing mechanisms (a) increased mixing of fuel–air promoting growth of ξ_{st} and (b) increased conditional scalar dissipation rate ($\chi|\xi_{st}$). A factor ϖ was proposed by Sreedhara and Lakshmisha (2002a) to determine relative strengths of these two effects. Lower value of ϖ favors earlier autoignition. Figure 10.4 shows a variation of ϖ with time in a 2D and a 3D DNS at two values of τ_t . Effect of decreasing τ_t on ϖ is opposite in a 2D and a 3D DNS. Also, value of ϖ in a 2D DNS is always higher than that in a 3D DNS. Therefore, the influence of decreasing τ_t is opposite in a 2D DNS and a 3D DNS. 3D turbulence promoted mixing due to the presence of vortex-stretching phenomenon in 3D turbulence, which is absent in 2D turbulence.

In spite of using different configurations as given in Table 10.1, several features of autoignition in a turbulent medium, such as autoignition spots originate at a mixture having most reactive mixture fraction and having low conditional scalar dissipation rate, remained the same. Effect of turbulence on ignition delay is also not influenced by the configuration of the problem. Ignition delay is mainly influenced by the regimes of autoignition, viz., mixing controlled regime or kinetics controlled regime.

10.3 Homogeneous Charge Compression Ignition Engine

Simultaneous reduction of NO_x and soot in conventional CI engines is a challenging goal. Higher temperatures promote formation of NO_x . In a conventional CI engine, a few well-mixed spots are present where temperature goes to high value and NO_x is formed. A few spots of fuel-rich mixtures may also exist where soot forms due to insufficient amount of oxidizer. Homogeneous charge compression ignition (HCCI) is being suggested as one of the strategies to overcome this problem (Yao et al. 2009). Fuel and air are well mixed, like in conventional SI

engine, before the combustion occurs in an HCCI engine. Because of premixing, formation of soot can be avoided. Also, lower equivalence ratio reduces NO_x emissions because of lower in-cylinder temperature. However, due to premixing of fuel–air, HCCI engine suffers from lack of control over combustion. Also, at higher loads, excessive pressure rise takes place which can damage the engine (Dec 2009). It may be noted that, if the fuel–air mixture is truly homogeneous, then the autoignition may be controlled solely by chemical kinetics. Since the kinetics is affected by pressure, temperature, and concentration of reactants, creating inhomogeneous mixture or stratification (in terms of local temperature and/or local equivalence ratio) may assist in controlling the combustion in an HCCI engine (Yao et al. 2009). Therefore, a few DNS studies on autoignition in a HCCI-like environment are discussed in the following section.

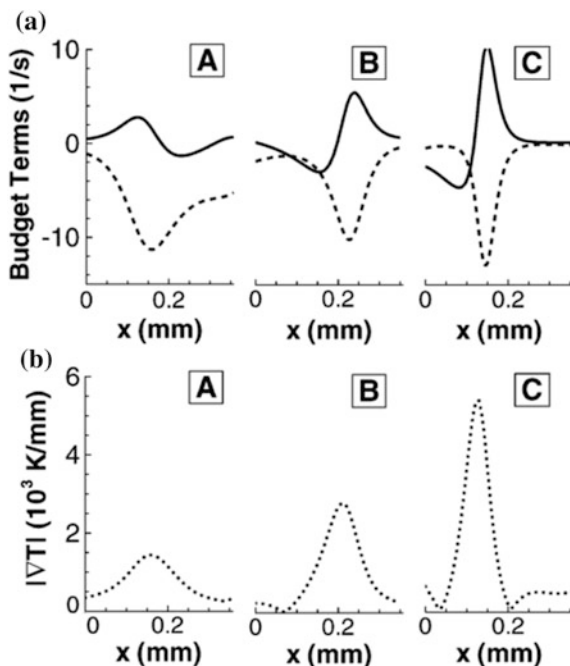
10.3.1 DNS of Combustion in HCCI Engines

Zeldovich (1980) identified two regimes of combustion in an inhomogeneous mixture (a) spontaneous ignition, where autoignition occurs successively at neighboring locations due to difference in autoignition delay time, which may appear like a propagating flame and (b) deflagration, where flame actually propagates in the mixture with reactive–diffusive balance. Zeldovich (1980) proposed that speed of this deflagration is inversely proportional to $|\nabla T|$. Possibility of deflagration in HCCI engine has been confirmed by experiments as well (for example, Kaiser et al. 2002). DNS studies of autoignition in HCCI-like environment also show this possibility of deflagration (Sankaran et al. 2005; Chen et al. 2006; Hawkes et al. 2006; Bansal and Im 2011). These studies highlight the importance of $|\nabla T|$ in determining the combustion regime. Therefore, it is of interest to study the factors which determine the regimes of combustion. Deflagration is characterized by a quantity called displacement speed given by Eq. (5), where ϕ is any reactive scalar (for example, one of the species mass fractions). Numerator in this equation is the sum of a diffusion and a reaction contribution to the propagation of the ϕ iso-contour. For deflagration in a purely premixed medium, balance between these two contributions should exist.

$$S_d = \frac{\nabla(\rho D_\phi \nabla \phi) + \dot{\omega}_\phi}{\rho |\nabla \phi|} \quad (5)$$

Figure 10.5 obtained by Chen et al. (2006), in a 2D DNS of ignition of inhomogeneous H_2 -air mixture, shows this reactive–diffusive balance at different locations (A, B, and C) in the domain. Reaction term is almost of a constant magnitude (H_2 is being consumed). Contribution of diffusion is increasing from location A to location C with increase in local temperature gradient. At very high temperature gradient (location C), reaction and diffusion terms are balancing each

Fig. 10.5 **a** Structure of reaction–diffusion balance for H_2 . Dashed line: Reaction, Solid line: Diffusion **b** local temperature gradient at different locations A, B, and C in the domain. Reprinted from Chen et al. (2006), by permission of Elsevier



other. Scatter plot of density weighted S_d , denoted by S_d^* ($S_d^* = \rho S_d / \rho_0$), and $|\nabla T|$ in the same study (not shown here) confirms the inverse relation between S_d^* and $|\nabla T|$. Here, ρ_0 is a representative density of the reactants. However, S_d^* did not decrease indefinitely but attained a value close to the laminar flame speed at high $|\nabla T|$. Also at low $|\nabla T|$, S_d^* increased sharply (5–6 times the laminar flame speed) indicating spontaneous ignition. Therefore, the magnitude of S_d^* was established as a criterion to distinguish between these two regimes. Hawkes et al. (2006) investigated the effect of increase in fluctuations of initial temperature field. With increase in temperature fluctuations, deflagration mode became more prominent. This was due to availability of increased value of $|\nabla T|$ in the domain. In these studies (Sankaran et al. 2005; Chen et al. 2006; Hawkes et al. 2006) equivalence ratio was uniform in the domain and only temperature fluctuations were considered. Bansal and Im (2011) performed 2D DNS of H_2 -air combustion wherein equivalence ratio fluctuations were also introduced. Two types of initial distributions were considered (a) uncorrelated temperature and equivalence ratio and (b) negatively correlated equivalence ratio and temperature. The case with uncorrelated field showed a deflagration mode whereas the case with negative correlation burned more homogeneously. Hence, it was concluded that combustion mode can be changed by changing initial correlation between temperature and equivalence ratio.

10.3.1.1 Heat Release Rate in HCCI Engine

As discussed previously, HCCI engine suffers from a drawback of excess pressure rise at higher loads. Pressure rise is controlled by the heat release rate during the combustion process. Therefore, heat release rate (HRR) in HCCI-like medium and factors influencing the HRR are discussed in this section. Introduction of stratification (temperature and/or equivalence ratio) extends the duration of HRR with lower peak values of HRR (Bansal and Im 2011; Yoo et al. 2011, 2013; Talei and Hawkes 2015). Due to the stratification, there are fewer sites which are about to autoignite at a given instant and this is responsible for prolonging the heat release. As discussed previously, Bansal and Im (2011) observed that the HRR profile in the negatively correlated temperature–equivalence ratio field was closer to the HRR observed in the homogeneous case. This was due to the absence of deflagration and hence homogeneous combustion occurred in the whole domain. Thus, the deflagration mode of combustion promotes smoothing of HRR.

Heavier hydrocarbons like *n*-Heptane show a two-stage ignition at lower initial temperatures. Also, there exists a negative temperature coefficient (NTC) regime where ignition delay increases with increase in initial temperature. Variation of ignition delay with temperature is shown in Fig. 10.6 for *n*-Heptane–air mixture. *n*-Heptane is used as a reference fuel to study autoignition and engine knock in CI engine, because the Cetane number of *n*-Heptane, approximately 56, is closer to that of commercially available diesel fuel (Curran et al. 1998). Yoo et al. (2011) studied the effect of temperature stratification on HRR at mean temperatures of 1008, 934, and 850 K (shown in Fig. 10.6).

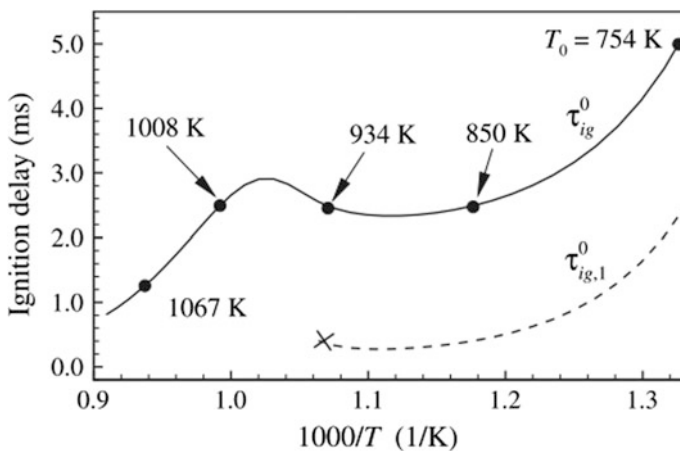


Fig. 10.6 Homogeneous ignition delay for *n*-Heptane–air mixture at constant volume and initial pressure of 40 bar as a function of initial temperature. Solid line: Stage two ignition delay, Dashed line: Stage one ignition delay. Reprinted from Yoo et al. (2011), by permission of Elsevier

For 1008 K case ignition delay decreased with increasing temperature stratification and an opposite trend was observed for 850 K case. 934 K case showed non-monotonic behavior. Also, the effect of stratification on 934 K, though a non-monotonic, was less pronounced compared to other two cases. Since the ignition delay is a function of initial temperature, a range of possible ignition delays exist in the domain based on the initial temperature distribution. It was shown that 1008 and 850 K case initially contained larger range of ignition delays. Since 934 K is located at the middle of NTC regime, it contained only a small range of ignition delays. This was the reason for less pronounced effect of stratification on 934 K case. Effect of stratification on low mean temperature case (754 K) was also not prominent because the turbulence could have homogenized the initial stratified field before the ignition occurred. The ratio τ_i/τ_0 was 0.5 in 754 K case. In another study, Yoo et al. (2013) investigated the effect of spark timing on combustion in a stratified medium using 2D DNS of *iso*-Octane-air mixture. Spark was provided in the form of high temperature zone at the center of the domain. Use of spark brought the ignition earlier. Pressure rise rate was smoother with earlier ignition. This was due to the deflagration wave started by the spark. However, the effect of spark timing on the pressure rise was not as noticeable as that observed with increase in temperature stratification. Yu and Bai (2013) investigated the effect of flow dimensionality (2D/3D) on the HRR in a stratified medium using DNS of H₂-air mixture. 3D case was found to ignite slightly later than 2D case and also heat release was more rapid in 3D case. As discussed in Sect. 10.2.1.1, in mixing controlled regime, 3D case brought about faster mixing of fuel-air. Temperature fluctuations in 3D case dropped faster than 2D case and hence the 2D case ignited earlier due to the presence few pockets having high temperature (Fig. 10b in Yu and Bai 2013). Stratified medium considered by Yu and Bai (2013) had uniform equivalence ratio and only temperature fluctuations were present. Also, due to better mixing in 3D case, heat release rate in the 3D case rises rapidly similar to that found in homogeneous combustion.

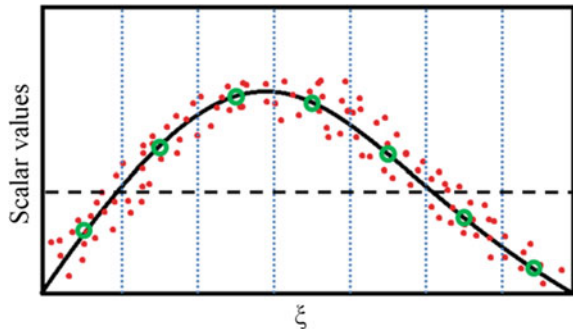
Talei and Hawkes (2015) performed 2D DNS of *n*-Heptane-air mixture with initial conditions like pressure, mean temperature, and mean equivalence ratio, almost same as those considered by Yoo et al. (2011). Talei and Hawkes (2015) considered stratification of initial equivalence ratio and maintained a negative correlation between initial temperature and equivalence ratio fields. Same reduced kinetic mechanism was used in both the studies. In all the cases considered by ignition occurred earlier with increasing temperature stratification. Equivalence ratio stratification was increased with temperature stratification by keeping their ratio constant. In the study by Yoo et al. (2011), the effect of increasing temperature stratification changed depending upon the mean initial temperature. Also, peak of heat release rate showed a non-monotonic behavior with increasing temperature stratification in the study by Talei and Hawkes (2015). Whereas, it decreased monotonically with increasing temperature stratification in the study by Yoo et al. (2011). Therefore, it can be said that an introduction of stratification in equivalence ratio along with temperature stratification changes the behavior of combustion in HCCI-like environment.

It may be noted from the above-reviewed publications that the stratification of temperature is a useful strategy in controlling the HRR in an HCCI engine. Temperature stratification promotes deflagration, which in turn, causes a smooth HRR in the domain. However, stratification of equivalence ratio along with that of temperature inhibits the deflagration mode of combustion. Temperature stratification inside combustion chamber is often created passively in an HCCI engine, resulting from mixing of bulk charge and boundary charge cooled by walls. Enhancing temperature stratification beyond naturally occurring stratification is a challenge (Dec 2009). Stratification of equivalence ratio may be controlled actively by controlling location and timing of injection of fuel.

10.4 Assessment of Conditional Moment Closure Model

Conditional moment closure (CMC) is one of the models proposed to capture turbulence–chemistry interaction without invoking any assumption on the flame structure. A discussion about CMC model and an assessment of its accuracy with DNS data has been presented in this section. The CMC model was independently proposed by Klimenko (1990) and Bilger (1993). It is well-known that variables like temperature, species mass fraction, fluctuate in time at a given location in a turbulent flow. CMC methodology assumes that these fluctuations can be associated with fluctuations of a single property, which is known as mixture fraction (ξ) in turbulent non-premixed combustion (Klimenko and Bilger 1999). The concept of CMC has been illustrated in Fig. 10.7. Figure 10.7 shows a scatter plot of a scalar Y and the mixture fraction ξ . Dashed line indicates an unconditional mean of Y . In CMC, mixture fraction space is divided into number of “bins” (or intervals) and the average of Y is calculated in that bin and is represented in Fig. 10.7 using hollow circles. It is called the conditional mean and denoted as $\langle Y|\xi = \eta \rangle$. It indicates the mean of values of Y subjected to the condition to the right of vertical line, i.e., $\xi = \eta$ is satisfied, where η is sample space of variable ξ . It may be clearly seen from Fig. 10.7 that the conditional fluctuations of Y are very small compared to unconditional fluctuations. In CMC, governing equations are solved for $\langle Y|\xi = \eta \rangle$.

Fig. 10.7 Scatter plot (\bullet) of a scalar Y and ξ . Solid line: Conditional mean of scalar Y conditioned on ξ , dashed line: Unconditional mean of scalar. \circ shows mean of respective bin



Variables calculated in the mixture fraction space are converted into variables in the physical space by using an appropriate probability density function of ξ . Discussion in this section closely follows Sreedhara (2002) and Sreedhara and Lakshmisha (2002a). CMC equations have been derived by Klimenko and Bilger (1999) in their review paper. In the next section, the CMC equations will be discussed.

10.4.1 CMC Equations

Governing equation of conditional mean of species mass fraction is given by Eq. (6). Q for any quantity is defined as $Q(\eta; x, t) = \langle Y|\eta \rangle$. In a spatially homogeneous and isotropic turbulence, advection terms vanish and momentum equations become zero after taking the average. Temperature is replaced by a suitably defined excess temperature $\theta = (T - T_{in})c_p/h_r$ where h_r is the heat of reaction. Governing equation of conditional mean of excess temperature is given by Eq. (7). Δh_α is the heat of formation of a species. In Eqs. (6)–(7), conditional mean of scalar dissipation rate ($\langle \chi|\eta \rangle$) and conditional mean of reaction rate ($\langle \dot{\omega}_\alpha|\eta \rangle$) require closure models. First, the model for reaction rate will be discussed.

$$\frac{\partial Q_\alpha}{\partial t} = \frac{1}{2} \langle \chi|\eta \rangle \frac{\partial^2 Q_\alpha}{\partial \eta^2} + \frac{1}{\rho} \langle \dot{\omega}_\alpha|\eta \rangle \quad (\alpha = 1, \dots, N_S) \quad (6)$$

$$\frac{\partial Q_\theta}{\partial t} = \frac{1}{2} \langle \chi|\eta \rangle \frac{\partial^2 Q_\theta}{\partial \eta^2} + \frac{1}{\rho h_r} \frac{\partial Q_p}{\partial t} - \frac{1}{\rho h_r} \sum_{\alpha=1}^{N_S} \Delta h_\alpha \langle \dot{\omega}_\alpha|\eta \rangle \quad (7)$$

Closure of reaction rate can be expressed in terms truncated series approximation, as given by Mastorakos and Bilger (1998). It is given by Eq. (8). Here, $\Theta_0(\eta) = T_{in}^2(\eta)c_p/T_a H_F$ and H_F is the heat of combustion of fuel. Quantity σ^2 is conditional variance of temperature $\langle \theta'^2|\eta \rangle$ where $\theta' = \theta - Q_\theta$. Additional governing equation for σ^2 is also given by Mastorakos and Bilger (1998) (not given here). Closure for conditional scalar dissipation rate has been given by Mell et al. (1994) and is given in Eq. (9).

$$\langle Y_\alpha Y_\beta \exp \frac{\theta}{\Theta_0(\eta)} |\eta \rangle = Q_\alpha Q_\beta \left[1 + \frac{\sigma^2}{2\Theta_0^2(\eta)} \right] \exp \frac{Q_\theta}{\Theta_0(\eta)} \quad (8)$$

$$\langle \chi|\eta \rangle = \chi_m \exp[-2\{erf^{-1}(2\eta - 1)\}^2] \quad (9)$$

Sreedhara and Lakshmisha (2002a) have given alternative closure models for reaction rate and scalar dissipation rate. Equation (8) involves assumption of small value of θ . However, this assumption breaks down during autoignition, especially during rapid heat release phase. Therefore, a new closure model was proposed which does not require this assumption. Instead, it assumes θ'' to be small which

holds good even during the rapid heat release phase. Final closure of reaction rate proposed by Sreedhara and Lakshmisha (2002a) is given in Eq. (10). Here $\Theta(\eta) = Q_T^2 c_P / T_a h_r$. Factor $\varphi_{\alpha\beta}$ has been introduced to take into account effects of species fluctuations and is given by Eq. (11). This factor was found to be important mainly when multistep chemistry was used. Model for $\varphi_{\alpha\beta}$ was also proposed by Sreedhara and Lakshmisha (2002b) (not given here). Equation (9) for conditional scalar dissipation rate assumes constant value of χ_m . However, based on DNS data of homogeneous decaying turbulence (Sreedhara and Lakshmisha 2000), it was observed that scalar dissipation rate decays with time (Fig. 6 in Sreedhara and Lakshmisha 2000, not shown here). This is true only for decaying turbulence. When the turbulence is externally forced, χ_m may remain constant. Therefore, $\chi_m = \chi_{m0} \exp(-2t/\tau_{t0})$ was proposed by Sreedhara and Lakshmisha (2002b). χ_{m0} and τ_{t0} are initial values of χ_m and integral timescale of the turbulence, respectively.

$$\langle Y_\alpha Y_\beta \exp \frac{\theta}{\Theta_0(\eta)} | \eta \rangle = \frac{Q_\alpha Q_\beta}{\varphi_{\alpha\beta}(\eta)} \left[1 + \frac{\varphi_{\alpha\beta}(\eta) \sigma^2}{2\Theta^2(\eta)} \right] \exp \left(\frac{-T_a}{Q_T} \right) \quad (10)$$

$$\varphi_{\alpha\beta}(\eta) = \frac{Q_\alpha Q_\beta}{\langle Y_\alpha Y_\beta | \eta \rangle} \quad (11)$$

10.4.2 Assessment of CMC Closure Models

Accuracy of CMC modeling was assessed by Sreedhara and Lakshmisha (2002b) using 3D DNS data related to autoignition of *n*-Heptane–air mixture. Single-step as well as four-step chemistry of *n*-Heptane–air was considered. Two types of CMC models, viz., CMC-I and CMC-II, were considered. $\langle \chi | \eta \rangle$ was modeled using Eq. (9) with χ_m being function of time in both the types of CMC.

- (1) $\sigma^2 = 0$ and $\varphi_{\alpha\beta} = 1$ was used while calculating conditional reaction rate (CMC-I).
- (2) σ^2 was obtained by solving its equation and model for $\varphi_{\alpha\beta}$ was used (CMC-II).

CMC-I ignores the effects of conditional temperature fluctuations and conditional species fluctuations.

Details of single-step and four-step chemistry used in Sreedhara and Lakshmisha (2002) are given in Tables 10.3, 10.4 and 10.5 for a quick reference. X and Y

Table 10.3 Single-step and four-step reaction mechanisms of *n*-C₇H₁₆–air

$n - C_7H_{16} + 11(O_2 + 3.76N_2) \rightarrow 8H_2O + 7CO_2 + 11 \times 3.76N_2 + \text{Heat}$	(S1)
$n - C_7H_{16} \rightarrow X$	(R1)
$X + 11O_2 \rightarrow P$	(R2)
$n - C_7H_{16} + 2O_2 \rightleftharpoons Y$	(R3F, R3B)
$Y + 9O_2 \rightarrow P$	(R4)

Table 10.4 Chemical kinetic parameters of reactions

Reaction	A (mm ³ /mol.s or 1/s)	T _a (K)
S1	4.1 × 10 ¹⁴	16000
R1	3.57 × 10 ⁸	21650
R2	7.14 × 10 ¹³	7220
R3F	1.07 × 10 ²⁰	21650
R3B	1.43 × 10 ²¹	37285
R4	1.78 × 10 ¹⁵	13230

Table 10.5 Heat of formation of species in the four-step mechanism

Species	n-C ₇ H ₁₆	X	O ₂	Y	P	N ₂
Δh _α (MJ/kg)	-22.04	-7.92	0.0	-12.61	-10.42	0.0

represent the molecular groups (3C₂H₄ + CH₃ + H) and (HO₂C₇H₁₃O + H₂O), respectively. P represents final products (7CO₂ + 8H₂O). Heat of combustion for single-step mechanism was taken as 29.67 MJ/kg of fuel.

10.4.2.1 Single-Step Chemistry

Figure 10.8 shows comparison between evolution of conditional temperature (at $\eta = \xi_{MR}$) with time as predicted by DNS and CMC. Both CMC-I and CMC-II models successfully predict the evolution of conditional temperature. Also, initial value of Da had no effect on the accuracy of both these models. Even CMC-I predicted the correct variation of ignition delay with variation in initial integral timescale, i.e., decrease in ignition delay time with decrease in initial integral timescale of turbulence. However, CMC-I predicted an opposite trend (increase in ignition delay time with decrease in initial integral timescale of turbulence) to that observed in DNS when χ_m was kept constant. Also, deviation between CMC-I and CMC-II became prominent at higher initial values of χ_{m0} .

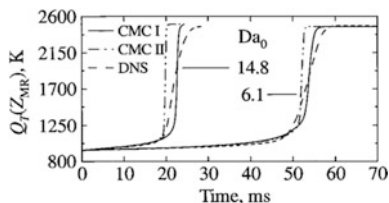


Fig. 10.8 Variation of conditionally averaged temperature with time at two different initial Da . Mixture fraction ξ denoted by Z in this figure. Reprinted from Sreedhara and Lakshmisha (2002), by permission of the Combustion Institute

10.4.2.2 Four-Step Chemistry

When multistep chemistry was used, CMC-I predictions deviated from the DNS data, whereas prediction of CMC-II was still in agreement with the DNS data. The value of the factor $\varphi_{\alpha\beta}$ was evaluated by comparing it against the data obtained from DNS. Its value was indeed found to be more than 1 for X-O pair when multistep chemistry was used. However, it was found to be 1 for single-step chemistry. Therefore, the effect of fluctuations in species mass fraction cannot be neglected in the problems involving multistep chemistry.

10.5 Conclusions

Several DNS studies of autoignition in a turbulent non-premixed medium were discussed in this chapter. Combustion in HCCI engine as an extension of conventional CI engines was also discussed. Finally, the use of DNS data in assessing the accuracy of closure models was presented. Major findings may be summarized as follows:

- (1) Fluid dynamic effects on autoignition in laminar as well as in turbulent flows cannot be neglected. These effects become more important in turbulent medium where variables are fluctuating with time.
- (2) DNS data has shown that autoignition in a turbulent non-premixed medium occurs when two conditions are jointly satisfied (i) mixture fraction attains a value of most reactive mixture fraction and (ii) conditional scalar dissipation rate is low. Also, with respect to fluid dynamic structures, autoignition spots appear at the vorticity dominated cores of vortices and combusting gases move toward the strain-dominated periphery.
- (3) Most DNS studies on autoignition referred in this chapter relied on simplified chemistry and single-stage autoignition. However, few studies considering two-stage autoignition using multistep chemistry were also discussed. Location of autoignition spots relative to local vortical structure was found to be similar in both types of studies.
- (4) Two regimes of autoignition can be identified (i) mixing controlled and (ii) kinetics controlled. In the mixing controlled regime, rate of mixing controls the rate of reaction. Integral timescale is shorter than the characteristic ignition delay in this regime. In the kinetics controlled regime, integral timescale is longer than the characteristic ignition delay and a few well-mixed spots are sufficient to start combustion. Influence of integral timescale on ignition delay depends on these regimes of combustion.
- (5) 2D DNS predicts an increase in ignition delay with decrease in integral timescale which contradicts experimental observations. 3D DNS settles this contradiction and predicts decrease in ignition delay with decrease in integral

timescale. The mechanism of vortex-stretching is responsible for this discrepancy between 2D and 3D DNS.

- (6) Homogeneous charge compression ignition engine is an improvement over the conventional CI engine. Control of start of combustion in a truly homogeneous mixture of fuel–air is not possible and therefore the stratification is introduced in the mixture. DNS study of autoignition in HCCI-like medium reveals a possibility of the deflagration mode of combustion, which can smoothen the heat release rate. Correlation between initial equivalence ratio and temperature fields also affects the heat release rate.
- (7) Data obtained from a DNS may be used to assess the accuracy of closure models used in RANS/LES. This application of DNS was demonstrated using study of the CMC model. If the right model for the scalar dissipation rate is used, first-order CMC can produce accurate results. However, with multistep chemistry, first-order CMC is inadequate.

Acknowledgements Most of these works were carried out by one of the authors, during his PhD, under the supervision of Prof. K. N. Lakshmisha, IISc, Bangalore.

References

- Bansal G, Im HG (2011) Autoignition and front propagation in low temperature combustion engine environments. *Combust Flame* 158:2105–2112. <https://doi.org/10.1016/j.combustflame.2011.03.019>
- Bilger RW (1993) Conditional moment closure for turbulent reacting flow. *Phys Fluids A Fluid Dyn* 5:436–444. <https://doi.org/10.1063/1.858867>
- Cabra R, Myhrvold T, Chen J-Y et al (2006) Simultaneous laser raman-rayleigh-lif measurements and numerical modeling results of a lifted turbulent H₂/N₂ jet flame in a vitiated coflow. *Combust Sci Technol* 178:1001–1030. <https://doi.org/10.1080/00102200500270106>
- Chen JH, Hawkes ER, Sankaran R et al (2006) Direct numerical simulation of ignition front propagation in a constant volume with temperature inhomogeneities: I fundamental analysis and diagnostics. *Combust Flame* 145:128–144. <https://doi.org/10.1016/j.combustflame.2005.09.017>
- Curran HJ, Gaffuri P, Pitz WJ, Westbrook CK (1998) A comprehensive modeling study of n-Heptane oxidation. *Combust Flame* 114:149–177. <https://doi.org/10.1002/kin.20036>
- Dec JE (2009) Advanced compression-ignition engines—understanding the in-cylinder processes. *Proc Combust Inst* 32 II:2727–2742. <https://doi.org/10.1016/j.proci.2008.08.008>
- Fotache CG, Kreutz TG, Law CK (1997) Ignition of counterflowing methane versus heated air under reduced and elevated pressures. *Combust Flame* 108:442–470. [https://doi.org/10.1016/S0010-2180\(97\)81404-6](https://doi.org/10.1016/S0010-2180(97)81404-6)
- Hawkes ER, Sankaran R, Pebay PP, Chen JH (2006) Direct numerical simulation of ignition front propagation in a constant volume with temperature inhomogeneities: II Parametric study. *Combust Flame* 145:145–159. <https://doi.org/10.1016/j.combustflame.2005.09.018>
- Heywood JB (1988) *Internal combustion engine fundamentals*. McGraw Hill Education
- Hilbert R, Thévenin D (2002) Autoignition of turbulent non-premixed flames investigated using direct numerical simulations. *Combust Flame* 128:22–37. [https://doi.org/10.1016/S0010-2180\(01\)00330-3](https://doi.org/10.1016/S0010-2180(01)00330-3)

- Im HG, Chen JH, Law CK (1998) Ignition of hydrogen-air mixing layer in turbulent flows. *Symp Combust* 27:1047–1056. [https://doi.org/10.1016/S0082-0784\(98\)80505-5](https://doi.org/10.1016/S0082-0784(98)80505-5)
- Im HG, Chen JH, Chen JY (1999) Chemical response of methane/air diffusion flames to unsteady strain rate. *Combust Flame* 118:204–212. [https://doi.org/10.1016/S0010-2180\(98\)00153-9](https://doi.org/10.1016/S0010-2180(98)00153-9)
- Im HG, Raja L, Kee RJ, Petzold LR (2000) A numerical study of transient ignition in a counterflow nonpremixed methane-air flame using adaptive time integration. *Combust Sci Technol* 158:341–363. <https://doi.org/10.1080/00102200008947340>
- Kaiser EW, Yang J, Culp T et al (2002) Homogeneous charge compression ignition engine-out emission-does flame propagation occur in homogeneous charge compression ignition? *Int J Engine Res* 3:185–195. <https://doi.org/10.1243/146808702762230897>
- Klimenko AY (1990) Multicomponent diffusion of various admixtures in turbulent flow. *Fluid Dyn* 25:327–334. <https://doi.org/10.1007/BF01049811>
- Klimenko A, Bilger RW (1999) Conditional moment closure for turbulent combustion. *Prog Energy Combust Sci* 25:595–688
- Krisman A, Hawkes ER, Talei M et al (2016) A direct numerical simulation of cool-flame affected autoignition in diesel engine-relevant conditions. *Proc Combust Inst* 0:1–9. doi:<https://doi.org/10.1016/j.proci.2016.08.043>
- Krisman A, Hawkes ER, Chen JH (2017) Two stage autoignition and edge flames in a high pressure turbulent jet. *J Fluid Mech* 824:5–41. <https://doi.org/10.1017/jfm.2017.282>
- Liñán A, Crespo A (1976) An asymptotic analysis of unsteady diffusion flames for large activation energies. *Combust Sci Technol* 14:95–117. <https://doi.org/10.1080/00102207608946750>
- Mastorakos E (2009) Ignition of turbulent non-premixed flames. *Prog Energy Combust Sci* 35:57–97. <https://doi.org/10.1016/j.pecs.2008.07.002>
- Mastorakos E, Bilger RW (1998) Second-order conditional moment closure for the autoignition of turbulent flows. *Phys Fluids* 10:1246–1248. <https://doi.org/10.1063/1.869652>
- Mastorakos E, Baritaud TA, Poinot TJ (1997) Numerical simulations of autoignition in turbulent mixing flows. *Combust Flame* 109:198–223. [https://doi.org/10.1016/S0010-2180\(96\)00149-6](https://doi.org/10.1016/S0010-2180(96)00149-6)
- Mell WE, Nilsen V, Kosály G, Riley JJ (1994) Investigation of closure models for nonpremixed turbulent reacting flows. *Phys Fluids* 6:1331–1358. <https://doi.org/10.1063/1.868443>
- Mizutani Y, Kazuyoshi N, Jin Do C (1990) Effects of turbulent mixing on spray ignition. *Proc Combust Inst* 1455–1460
- Moin P, Mahesh K (1998) Direct numerical simulation: a tool in turbulence research. *Annu Rev Fluid Mech* 30:539–578. <https://doi.org/10.1146/annurev.fluid.30.1.539>
- Mukhopadhyay S, Abraham J (2012) Influence of turbulence on autoignition in stratified mixtures under compression ignition engine conditions. *Proc Inst Mech Eng Part D J Automob Eng* 227:748–760. <https://doi.org/10.1177/0954407012459624>
- Peters N (2004) *Turbulent combustion*. Cambridge University Press
- Poinot TJ, Veyante D (2005) *Theoretical and numerical combustion*, 2nd ed. Edwards
- Sankaran R, Im HG, Hawkes ER, Chen JH (2005) The effects of non-uniform temperature distribution on the ignition of a lean homogeneous hydrogen-air mixture. *Proc Combust Inst* 30:875–882. <https://doi.org/10.1016/j.proci.2004.08.176>
- Sreedhara S (2002) Studies on autoignition in a turbulent nonpremixed medium using direct numerical simulations. PhD Thesis, Indian Institute of Science
- Sreedhara S, Lakshmisha KN (2000) Direct numerical simulation of autoignition in a non-premixed, turbulent medium. *Proc Combust Inst* 28:25–33. [https://doi.org/10.1016/S0082-0784\(00\)80191-5](https://doi.org/10.1016/S0082-0784(00)80191-5)
- Sreedhara S, Lakshmisha KN (2002a) Autoignition in a non-premixed medium: DNS studies on the effects of three-dimensional turbulence. *Proc Combust Inst* 29:2051–2059. [https://doi.org/10.1016/S1540-7489\(02\)80250-4](https://doi.org/10.1016/S1540-7489(02)80250-4)
- Sreedhara S, Lakshmisha KN (2002b) Assessment of conditional moment closure models of autoignition using DNS data. *Proc Combust Inst* 29:2069–2077
- Talei M, Hawkes ER (2015) Ignition in compositionally and thermally stratified n-heptane/air mixtures: a direct numerical simulation study. *Proc Combust Inst* 35:3027–3035. <https://doi.org/10.1016/j.proci.2014.09.006>

- Yao M, Zheng Z, Liu H (2009) Progress and recent trends in homogeneous charge compression ignition (HCCI) engines. *Prog Energy Combust Sci* 35:398–437. <https://doi.org/10.1016/j.pecs.2009.05.001>
- Yoo CS, Richardson ES, Sankaran R, Chen JH (2011a) A DNS study on the stabilization mechanism of a turbulent lifted ethylene jet flame in highly-heated coflow. *Proc Combust Inst* 33:1619–1627. <https://doi.org/10.1016/j.proci.2010.06.147>
- Yoo CS, Lu T, Chen JH, Law CK (2011b) Direct numerical simulations of ignition of a lean n-heptane/air mixture with temperature inhomogeneities at constant volume: Parametric study. *Combust Flame* 158:1727–1741. <https://doi.org/10.1016/j.combustflame.2011.01.025>
- Yoo CS, Luo Z, Lu T et al (2013) A DNS study of ignition characteristics of a lean iso-octane/air mixture under HCCI and SACI conditions. *Proc Combust Inst* 34:2985–2993. <https://doi.org/10.1016/j.proci.2012.05.019>
- Yu R, Bai XS (2013) Direct numerical simulation of lean hydrogen/air auto-ignition in a constant volume enclosure. *Combust Flame* 160:1706–1716. <https://doi.org/10.1016/j.combustflame.2013.03.025>
- Zeldovich YB (1980) Regime classification of an exothermic reaction with nonuniform initial conditions. *Combust Flame* 39:211–214. [https://doi.org/10.1016/0010-2180\(80\)90017-6](https://doi.org/10.1016/0010-2180(80)90017-6)